Factors Influencing the Cold Transportation Process of Waxy Shale Oil

Hao Wan [1], Minfeng Tao [1], Chengjie Xie [1], Qiyu Huang [2], Yan Liang [1], Zhongqing Tang [1], Junlei Wang [1]✉

1. Sinopec Petroleum Engineering Jianghan Co., Ltd., Wuhan, 430000, China

2. School of Mechanical and Storage Transportation Engineering, China University of Petroleum, Beijing, 100000, China

✉**Correspondence author: Junlei Wang**

Authors Email:

Hao Wan: wanhao.osec@sinopec.com

Minfeng Tao: minfengt@163.com

Chengjie Xie : xiechengjie.osec@sinopec.com

Qiyu Huang : ppd@cup.eud.cn

Yan Liang: liangyan.osec@sinopec.com

Zhongqing Tang: 1520406382@qq.com

Junlei Wang: wangjl0321@163.com

Abstract: During the cold flow transportation (cold transportation) process of waxy crude oil, when the transportation temperature is below the wax precipitation point, wax deposition and pipe congealing phenomena can easily occur, affecting the safety of the transportation pipeline. By analyzing the microscopic wax crystal structure and size in the oil matrix under the cold transportation conditions of waxy shale oil, studying the rheological change rules of congealed oil during cold transportation, and combining basic physical properties with annular wax deposition simulation, a wax deposition kinetic model is developed. This model predicts the wax deposition rate and proposes safe transportation conditions and pipe cleaning requirements for cold transporting waxy shale oil. The results show that under cold transportation conditions, waxy shale oil forms needle-shaped microcrystalline wax with a length of less than 2 μm. Shear forces can disrupt the stable congealed oil structure and improve its rheological properties. Decreasing the initial temperature of cold transport helps reduce the yield stress of congealed oil. The kinetic model predicts a maximum wax deposition rate of no more than 0.23 mm/d. These findings can provide technical guidance for a flow safety design of the cold transportation process for waxy shale oil.

Introduction

Most waxy shale oils are light or medium crude oils with higher pour points, high wax content, and fewer asphaltenes and resins [1-3]. Wax deposition and pipe congealing commonly occur during low-temperature transportation, leading to reduced effective pipeline area and increased production energy consumption. In severe cases, it can cause pipe blockage, rupture, and equipment malfunction, significantly affecting pipeline operational safety [4-5]. To ensure the safe and smooth operation of the transport pipelines, domestic and international waxy shale oil and gas transport processes often adopt heating, fluid blending, and hot water accompanying thermal procedures, which are energy-intensive and require significant investments [6-7]. The transport technology for waxy shale oil and gas has significantly advanced with the continuous practice and increasing understanding of unconventional oil and gas surface engineering. Domestically, the Changqing Oilfield adopts an integrated well platform sled-mounted equipment seasonal heating single-pipe transport process, achieving unheated single-pipe transport under high water content, high gas-to-oil ratio, and short transportation radius conditions [8]. Internationally, Eagle Ford shale oil uses a single-pipe heated transport process

[9]. Therefore, researching the cold transportation process of waxy shale oil and gas below the wax precipitation point [10-12], enhancing transport system efficiency, saving energy, and simplifying the process is of great significance for efficient shale oil and gas resource development.

The cold transport process refers to the oil entering the transport pipeline at a temperature below its wax precipitation point. The formed microcrystalline wax is suspended in the oil matrix, and when the temperature drops below the pour point, solid wax crystals start to form. However, there is limited wax deposition, ensuring safe transportation with a stable congealed oil structure [13]. Factors affecting the safe transport of high pour point waxy oil include not only transport temperature, pressure, water content, and gas-to-oil ratio but primarily properties like base characteristics under low-temperature flow conditions, congealed oil structure stability and rheology, wax content, wax crystal structure size, and wax deposition rate [14-15]. Wax content, related to shale oil reservoir geological characteristics, is the main indicator affecting pour point and rheology. The rheology of waxy oil includes pour point, dynamic viscosity, and yield stress [16], reflecting the influence of wax crystal structure and quantity. The pour point is important reference data for determining the terminal inlet temperature of waxy oil transportation pipelines [17-18]. Dynamic viscosity represents the fluidity of oil in a cold environment [19, 20]. It is related to the amount of precipitated wax, wax crystal structure and quantity, cooling rate, thermal history, shear rate, and shear history [21, 22]. Wax deposition rate reflects the combined effects of transport temperature, dynamic viscosity, pipeline heat loss, and flow rate under flowing conditions [23-25]. The yield stress of congealed oil reflects structural strength under cold flow conditions and is the minimum pressure requirement for restarting congealed oil after shutdown [26, 27]. The main difference between waxy shale oil and waxy crude oil is that waxy shale oil has a higher wax content and fewer asphaltenes and resins. Among these, wax content and carbon number distribution determine the pour point [28], and asphaltenes and resins primarily affect viscosity [29]. Therefore, light or medium waxy shale oils with good cold flowability are essential for the implementation of cold transport processes.

For the Fuxing region, the representative well for high-wax shale oil is Taiye 1HF, with a pour point of 19°C, a density of 771 kg/m^3 (20°C), a wax content of 22.4%, a wax precipitation point of 29.3°C, and a wax peak point of 19.6°C. The shale oil and gas transportation system adopts a cold transport process, starting at around 25°C, with winter ground temperatures around 10°C. The terminal transportation temperature is as low as 17°C, ensuring the safe transportation of waxy shale oil. In order to ensure safe flow during the cold transport of waxy shale oil in the Fuxing region, this study examines the following: the structure and size of the wax crystals, the congealed oil yield stress, and the dynamic viscosity changes under cold transport conditions. It also develops a model to predict the rates of wax deposition and investigates the effects of cold transport on the rheological properties of congealed oil and wax deposition.

1 Microstructure of Paraffin Wax

Experimental Method: A preheated cell scraper is used to pick up a certain amount of the Taiye 1HF shale oil sample. It is quickly placed over a glass slide, and the oil sample is spread at a certain rate to ensure it is evenly applied to the slide. Then, the thickness of the oil film is assessed. The polarizing microscope and digital camera parameters are standardized. Adjustments are made to the microscope to observe the oil sample on the glass slide, and images are taken.

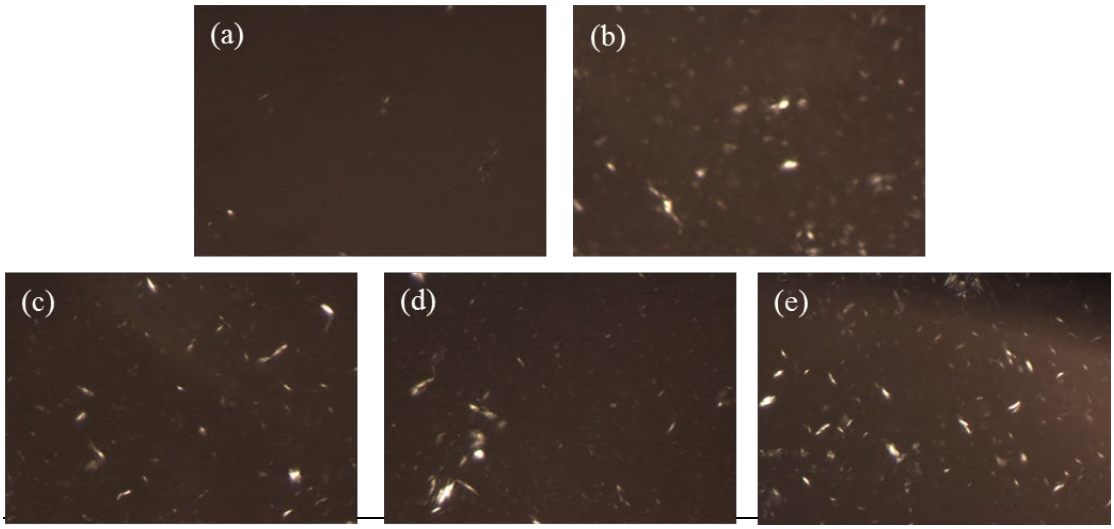

Fig. 1 The microstructure of shale oil in Taiye 1HF at 28°C, 25°C, 22°C, 20°C, and 19°C

As the temperature decreases, the amount of wax precipitating from the shale oil increases (Fig. 1), and both the size and perimeter of the wax crystals continue to grow (Table 1). Based on the length-width ratio of the wax crystals, it can be deduced that they are needle-shaped. The network structure formed by the aggregation of needle-shaped wax crystals is unstable and can be easily destroyed. Microcrystalline waxes formed below the wax precipitation point have lengths of less than 2 μm and equivalent diameters of less than 8 μm. Moreover, microcrystalline waxes have good dispersibility and can be stably suspended in shale oil, which is advantageous for cold transportation.

Table 1 Microscopic size of wax crystal in Taiye 1HF shale oil at different temperatures

Temperature °C	Length-Width Ratio	Size/μm^2	Perimeter/μm	Length/μm	Equivalent Diameter/μm
28	1.4	0.5	1.8	0.5	1.1
25	1.5	2.1	2.5	0.8	3.4
22	1.5	4.4	3.4	1.0	5.2
20	1.5	6.1	5.4	1.6	4.5
19	1.6	13.0	6.6	2.0	7.9

2 Change in the Rheological Properties of Gelled Oil

Apart from the gel point, the yield stress and dynamic viscosity of the gelled oil mainly represent the rheological properties of waxy shale oil[30]. An RS150H rheometer is used to test the yield stress of shale oil at different temperatures and the gelled oil viscosity at different shear rates.

Experimental Method: 1）Take the Taiye 1HF well oil sample and stir it in a high-pressure sealed stirring tank. Then, heat it up to 65°C and stabilize for 1 hour. After that, cool it down to the specified temperature at a constant rate, stirring continuously. 2）Set the water bath temperature of the RS150H rheometer to the specified temperature. 3）Set the rotor shear rate and experimental temperature (16°C, 13°C, and 10°C) and maintain a constant cooling rate. After reaching the target temperature, allow it to rest for varying durations: 1 h, 3 h, 6 h, 9 h, and 12 h. 4）At the designated time, consecutively set the shear rate to 10 1/s, 20 1/s, 30 1/s, 40 1/s, and 50 1/s to test the gelled oil's yield stress and viscosity under flowing conditions.

2.1 Yield Stress of Gelled Oil

2.1.1 Yield stress of gelled oil cooled statically from above the gel point to near ambient temperature.

The yield stress results after eliminating shear and thermal history are shown in Fig. 2a. The yield stress gradually increases as the temperature decreases and the gel point rises sharply below 4°C. The yield stress reaches 88.52 kPa at 10°C. The above condition indicates that as the pipeline transport temperature decreases, the shear force required to push the oil flow increases, especially below the gel point. In order to determine the yield stress changes under static cooling conditions with different static times, the static cooling temperatures are set to 16°C, 13°C, and 10°C and held for certain periods before testing the gelled oil's yield stress (Fig. 2b).

The yield stress of gelled oil increases with decreasing static temperature. For example, the yield stresses observed

after 1 h at 16°C, 13°C, and 10°C are 12.53 Pa, 37.12 Pa, and 86.56 Pa, respectively. Since the sampling and starting temperatures of the oil are both above the wax precipitation point, the oil is cooled at a constant rate to form a uniform and stable structure. As the temperature decreases, the oil's structure stability increases, and the shear force required to break the gelled oil structure and promote its flow increases. The gelled oil's yield stress tends to stabilize with prolonged static time, such as the yield stress after 1 h at 16°C being 12.53 Pa and after 12 h being 13.11 Pa.

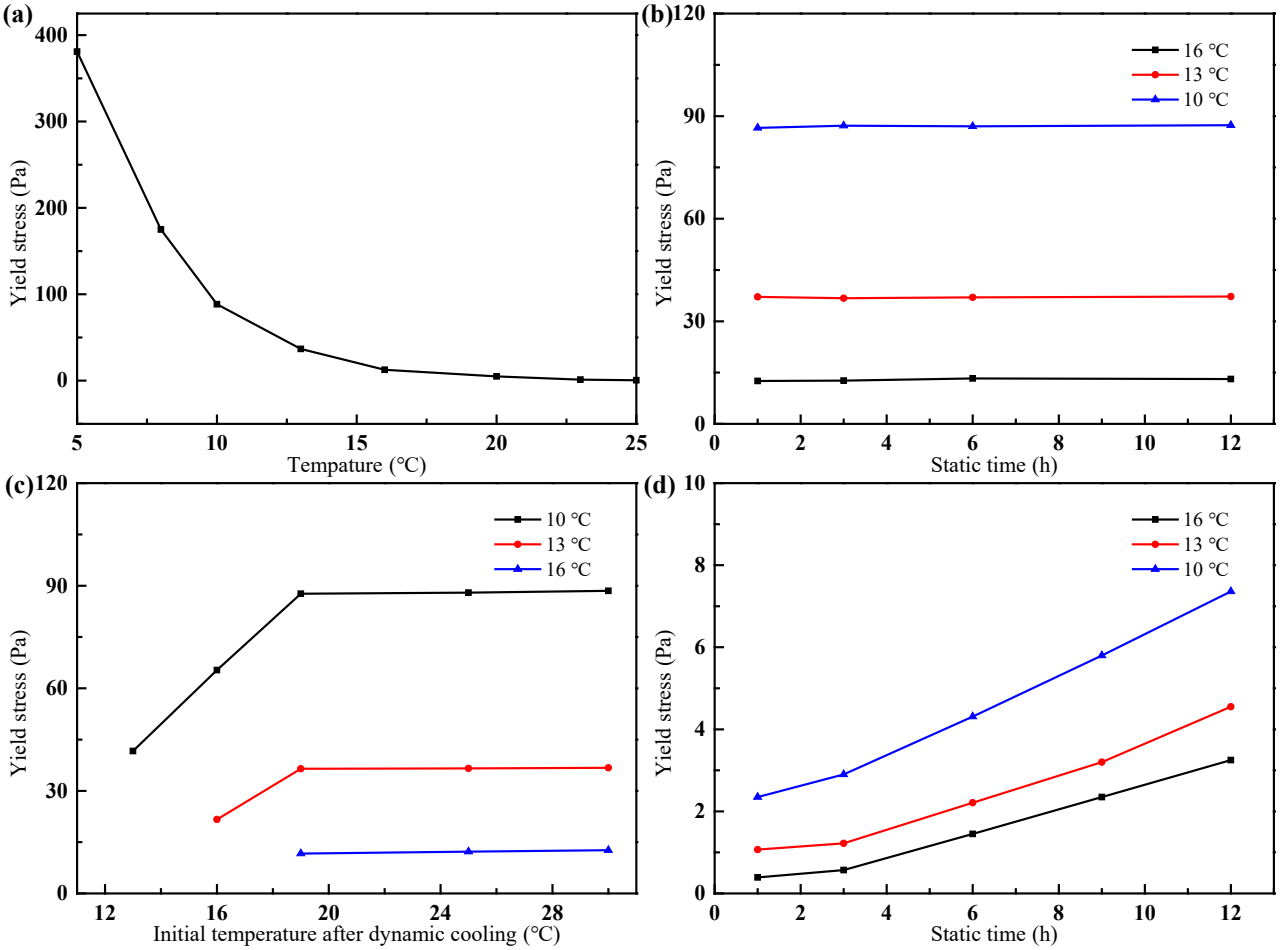

Fig. 2 The relationship between of yield stress and (a) shale oil temperature, (b) static time under static cooling conditions, (c) initial temperature after dynamic cooling to different temperatures, (d) static time after dynamic cooling to static temperature

2.1.2 Yield stress of gelled oil statically cools from a temperature between the gel point and ambient temperature to near ambient temperature.

Gelled oil, sheared, and cooled with the rotor dynamically at a constant rate (0.25°C/min) to 19°C, 16°C, and 13°C. Then, it is statically cooled to 10°C, 13°C, and 16°C, stabilized for 1 h, and the gelled oil's yield stress is tested (Fig. 2c).

After dynamic cooling and continued static cooling, the yield stress of the gelled oil decreases as the initial static cooling temperature drops. The yield stresses when the gelled oil is cooled from 19°C to 10°C and 13°C are 87.66 Pa and 36.48 Pa, respectively. When the gelled oil is cooled from 16°C to 10°C and 13°C, the yield stresses are 65.33 Pa and 21.63 Pa, respectively. The change in the yield stress is because the shear effect of the rotor under dynamic cooling conditions always destroys the gelled oil structure. Once the rotor stops and there is no shearing, the gelled oil structure recovers during static cooling. Therefore, lowering the initial static cooling temperature helps reduce the yield stress of the gelled oil, reducing the risk of pipeline stoppage and restart.

2.1.3 Stable yield stress of gelled oil near ambient temperature

Gelled oil dynamically sheared and cooled with the rotor at a rate of 0.25°C/min to 16°C, 13°C, and 10°C. It is then held for 1 h, 3 h, 6 h, 9 h, and 12 h, and the gelled oil's yield stress is tested (Fig. 2d).

Under dynamic cooling conditions, the gelled oil's yield stress rises as the static temperature drops. The decreasing temperature makes the waxy shale oil more susceptible to forming a uniform and stable gelled oil structure. Under dynamic cooling conditions, the shearing effect damages the oil structure, resulting in the yield stress of the gelled oil at

the same static temperature. However, the time is significantly lower than the yield stress of the gelled oil under static cooling conditions. The yield stress of the gelled oil increases with prolonged static time because the rotor is stationary and no longer continuously applying shear to the gelled oil structure. Also, the internal structure of the gelled oil is gradually recovering over time.

2.2 Dynamic Viscosity of Waxy Crude Oil

2.2.1 The Impact of Wax Crystals on the Dynamic Viscosity of Waxy Crude Oil

The dynamic viscosity under cold transport conditions significantly affects the low-temperature flow ability[31-33]. The RS150H rheometer was used to test the dynamic viscosity of shale oil at different shear rates and a cooling rate of 0.25℃/min, as shown in Fig. 3.

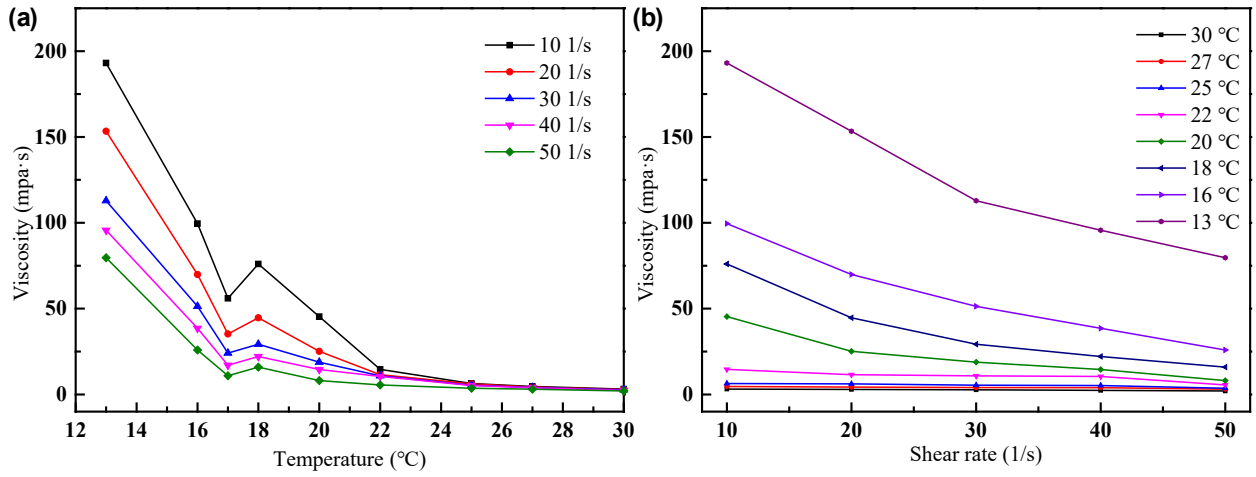

Fig. 3 The shale oil viscosity and (a) temperature curve, (b) shear rate curve

The dynamic viscosity of shale oil increases with the decrease in temperature (Fig. 3a). There is a rapid decrease in dynamic viscosity near the pour point under different shear rates. That happened due to the unstable network structure formed after the aggregation of needle-like wax crystals, which is easily destroyed by the rotor shear, leading to a rapid decrease in the dynamic viscosity of waxy shale oil near the pour point. Above the pour point, the viscosity of the oil is hardly affected by shear. However, below the pour point, applying minor shear stress causes the viscosity of the oil to decrease rapidly (Fig. 3b).

2.2.2 The Impact of Static Time on the Dynamic Viscosity of Waxy Crude Oil

The rotor was set to dynamically shear and cool at a rate of 0.25℃/min to 13℃. After static periods of 0 h, 1 h, 3 h, 6 h, 9 h, and 12 h, the waxy crude oil was then dynamically sheared at rates of 10 1/s, 20 1/s, 30 1/s, 40 1/s, and 50 1/s respectively, and the dynamic viscosity was tested, as shown in Fig. 4.

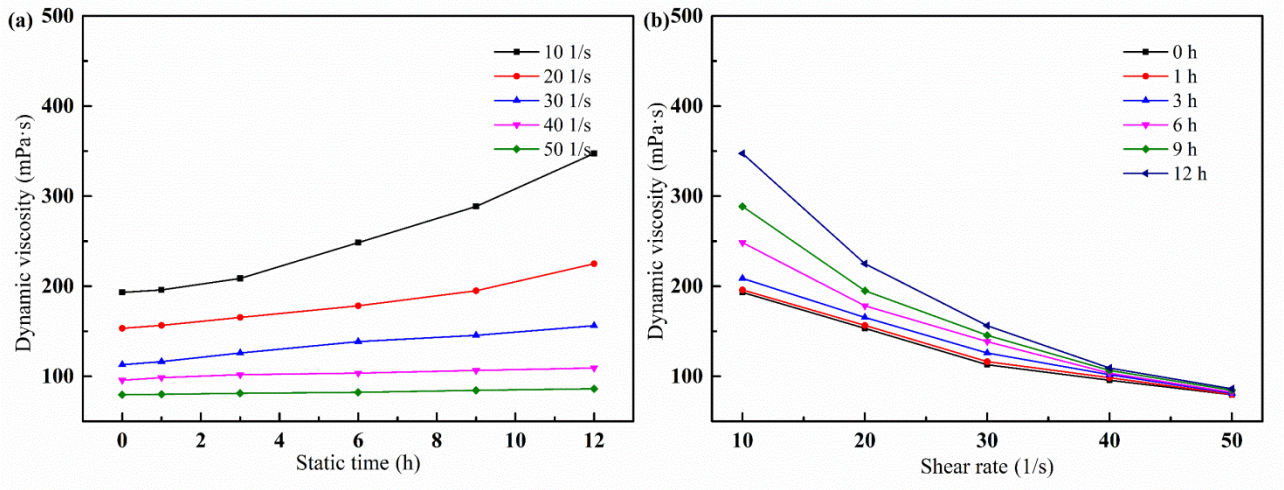

Fig. 4 (a) The relationship between dynamic viscosity and (a) static time, (b) shear rate after dynamic cooling to 13℃

The dynamic viscosity of cold waxy crude oil shows an increasing trend with the extension of static time (as shown in Fig. 4). The prolonged static time allows the waxy crude oil to form a more stable structure. At low shear rates, the viscosity of waxy crude oil shows a significant upward trend with static time. At high shear rates, the viscosity of waxy crude oil shows a stable trend because the structure of the waxy crude oil has been entirely destroyed under low shear rates, restoring its flowability, and the static time has a negligible effect on the viscosity of waxy crude oil under high shear rates. Therefore, applying low shear can destroy the structure of waxy crude oil.

3 Wax Deposition Rate and Prediction for Cold Transportation Pipelines

Based on the fundamental properties of shale oil and the annular wax deposition experimental simulation, a wax deposition kinetic model is constructed. This model can predict the wax deposition rate along the pipeline at different times, providing theoretical support for pipeline pigging in cold transport.

3.1 Wax Deposition Rate Kinetic Model

Experimental analysis of the deposition behavior of high-wax-containing shale oil from Fuxing under varying temperature differences between oil and wall, varying oil flow rates, and different temperature ranges of the oil wall adheres to the wax deposition model of China University of Petroleum (Beijing)[34-36].

$$W = k\tau_w^m \frac{1}{\mu}\frac{dC}{dT}\left(\frac{dT}{dr}\right)^n \qquad (3\text{-}1)$$

Where, W represents the wax deposition rate, g/(m^2·h); $\frac{dC}{dT}$ is the solubility coefficient of wax in oil, 1/°C; $\frac{dT}{dr}$ is the radial temperature gradient, °C/m; μ is the viscosity of oil, mPa·s; τ_w^m is the shear stress on the pipe wall, Pa. This model not only considers the diffusion effect of wax molecules on the deposition of wax on the pipe wall but also takes into account the impact of shear stress and oil flow scouring on the pipe wall, reflecting the influences of flow rate, temperature, temperature difference between oil flow and pipe wall, and oil flow scouring on wax deposition.

Considering the properties of shale oil, the key parameters k, m, and n in the model are solved and revised according to the annular wax deposition experimental results. In the annular wax deposition experiment, deposition time (13 h), oil flow velocity (0.33-0.77 m/s), pipe wall temperature (23-27°C), and oil flow temperature (28-32°C) were set.

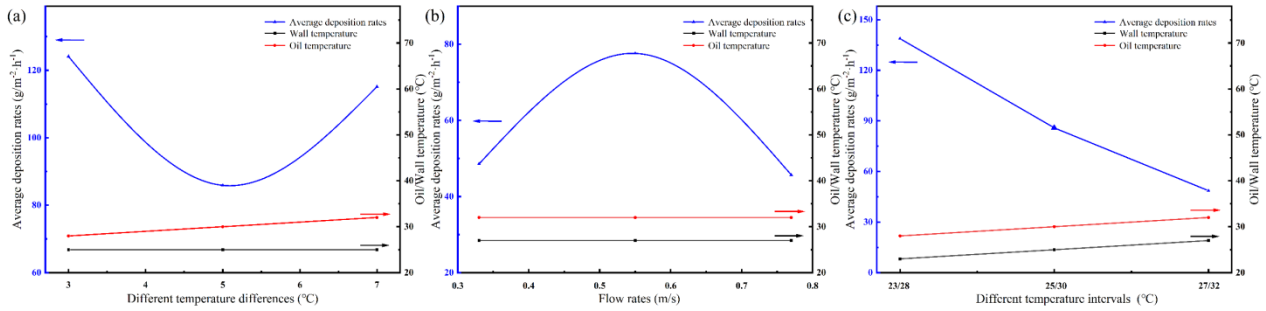

Fig. 5 The average deposition rates at (a) different temperature differences, (b) different oil flow rates, and (c) different temperature intervals

The wax deposition rate initially decreases, followed by an increase when the temperature difference between the oil and the wall increases. On the other hand, the wax deposition rate first increases and then decreases with the increase in the oil flow rate. Also, it gradually decreases with the following increase in the temperature zone of the oil wall. Based on the experimental test parameters of shale oil properties and annular experimental data, the parameters k, m, and n of the wax deposition rate model are adjusted and corrected, with k=27.4758, m=-0.26798, and n=-0.65764. The resulting wax deposition kinetic model for the waxy shale oil from the Fuxing area is as follows:

$$W = 27.4758\tau_w^{-0.26789}\frac{1}{\mu}\frac{dC}{dT}\left(\frac{dT}{dr}\right)^{0.34236} \qquad (3\text{-}2)$$

3. 2 Wax Deposition Rate Prediction

Based on the derived wax deposition kinetic model, the prediction software is developed in Matlab. Parameters like shale oil properties, pipe diameter, flow rate, oil temperature (30°C), and buried pipeline soil temperature (10°C) are used to determine the wax deposition rate at different times. Using the trial production data from the Fuxing area, the overall

heat transfer coefficient is calculated, and the wax deposition rates are computed for DN100, DN150, DN200, and DN250 at a minimum operating oil flow speed of 0.9 m/s.

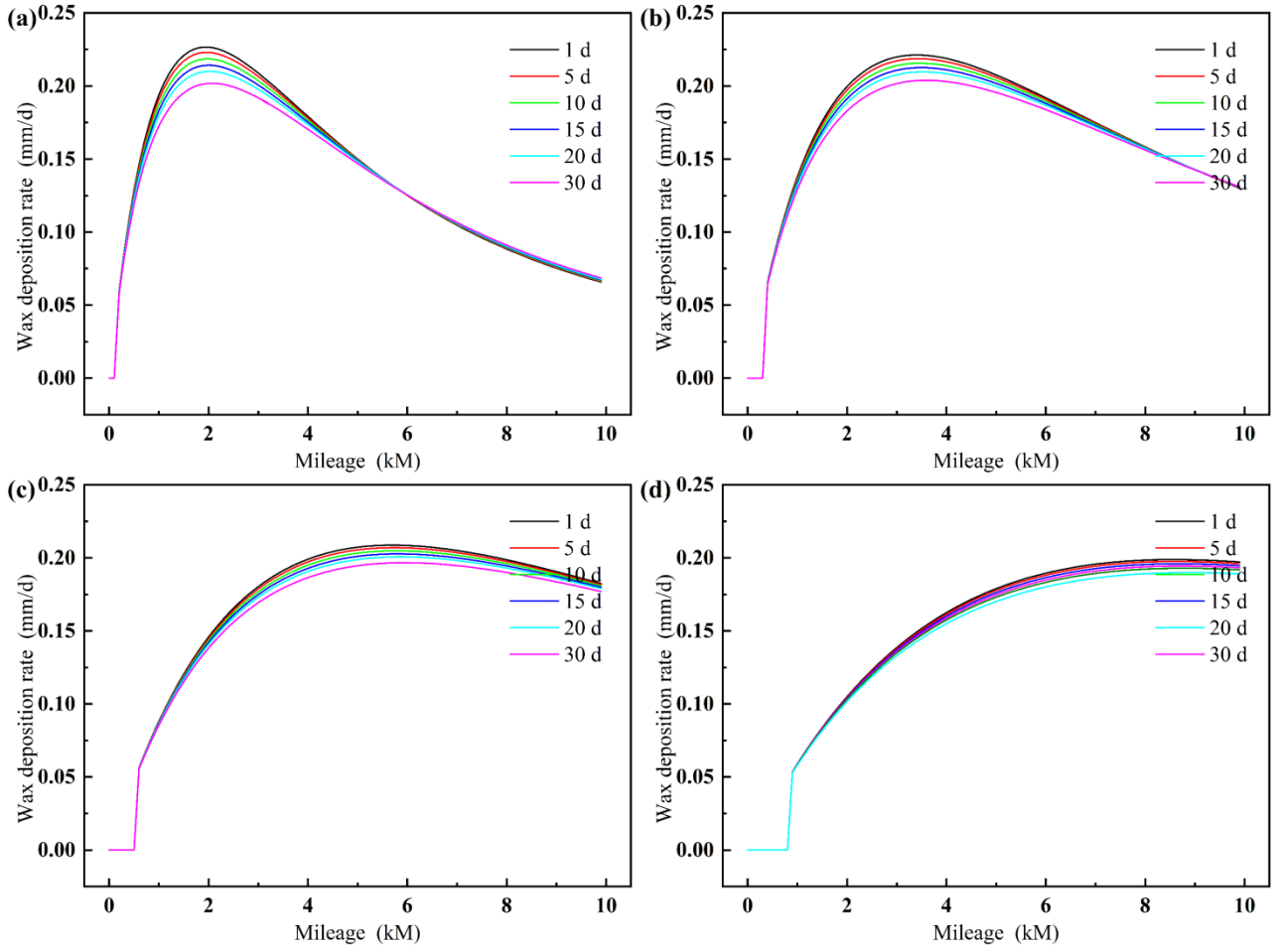

Fig. 6 The wax deposition rate of (a) DN100, (b) DN150, (c) DN200, (d) DN250

Wax deposition occurs when the pipeline temperature drops to the wax precipitation point (Fig. 6). As the length of the gathering and transportation pipeline increases, the wax deposition rate first increases and then decreases. As the diameter of the pipeline increases, the start position of wax precipitation extends from 0.1 km for DN100 to 0.8 km for DN250. The peak position of the wax deposition rate also shifts, and the deposition rate gradually decreases. The highest wax deposition rate occurs at 2.1 km on the first day of the DN100 pipeline operation, with a deposition rate of approximately 0.23 mm/d, while the DN250's maximum wax deposition rate is approximately 0.20 mm/d. As the operating time increases, the wax deposition rate gradually decreases, with the DN100 pipeline showing the most significant reduction, from 0.23 mm/d on the first day to 0.20 mm/d on the 30th day. Thus, the maximum wax deposition rate for shale oil gathering and transportation pipelines can be 0.23 mm/d.

4 Conclusions

The wax crystal structure of Fuxing waxy shale oil is the needle-shaped microcrystalline wax with a length-to-width ratio of 1.4-1.6. The needle-shaped microcrystalline wax length is less than 2 μm, and the equivalent diameter is less than 8 μm. The microcrystalline wax is stably suspended and dispersed in the oil matrix, making it favorable for cold transport and gathering processes.

The simulation of the changes in the yield stress of condensate under different cold transport conditions is

performed. First, when statically cooled from above the cloud point to near the ground temperature, the yield stress of the condensate rapidly rises as the temperature decreases and shows a stable trend with prolonged standing time. Second, when dynamically cooled to near ground temperature from a temperature between the cloud point and ground temperature, the yield stress of the condensate decreases with a decrease in the starting temperature of standing cooling. Third, near the ground temperature, the yield stress of the condensate decreases with the decrease in standing temperature and increases with prolonged standing time. A minor shear stress can break the stable condensate structure, facilitating cold transport flow.

Combining the basic properties of shale oil and the simulation results of loop wax deposition rules, the wax deposition kinetics model for Fuxing waxy shale oil is developed as $W = 27.4758\tau_w^{-0.26789}\frac{1}{\mu}\frac{dC}{dT}\left(\frac{dT}{dr}\right)^{0.34236}$. It predicts the wax deposition rate under cold transportation conditions for waxy shale oil. The maximum wax deposition rates for the gathering pipes DN100 and DN250 do not exceed 0.23 mm/d and 0.20 mm/d, respectively. The prediction results of the wax deposition rate for the cold transport gathering process can provide a theoretical basis for determining the pipeline cleaning cycle. In actual operations, the effects of dissolved gas, water content, and terrain elevation differences should be considered to adjust the cleaning cycle.

References

[1]. Chala G. T., Sulaiman S. A., Japper-Jaafar A.. Flow start-up and transportation of waxy crude oil in pipelines-A review[J]. Journal of non-newtonian fluid mechanics, 2018, 251: 69-87

[2]. Niu Z., Wang Y., Li Z., et al. Analysis of the Spatial Distribution Characteristics of Crude Oils with Different Freezing Points and the Genetic Mechanism of High-Freezing-Point Crude Oils in the Dongying Sag[J]. ACS omega, 2023, 8(38): 35093-35106.

[3]. Souas F., Safri A., Benmounah A. A review on the rheology of heavy crude oil for pipeline transportation[J]. Petroleum Research, 2021, 6(2): 116-136.

[4]. Alnaimat F., Ziauddin M.. Wax deposition and prediction in petroleum pipelines[J]. Journal of Petroleum Science and Engineering, 2020, 184: 106385.

[5]. El-Dalatony M. M., Jeon B. H., Salama E. S., et al. Occurrence and characterization of paraffin wax formed in developing wells and pipelines[J]. Energies, 2019, 12(6): 967.

[6]. Haruna A., Tanimu G., Ibrahim I., et al. Mitigating oil and gas pollutants for a sustainable environment–Critical review and prospects[J]. Journal of Cleaner Production, 2023: 137863.

[7]. Srinivasa Sai Abhijit Challapalli. (2024). Sentiment Analysis of the Twitter Dataset for the Prediction of Sentiments. Journal of Sensors, IoT & Health Sciences, *2*(4), 1-15.

[8]. Santos R. G. D., Loh W., Bannwart A. C., et al. An overview of heavy oil properties and its recovery and transportation methods[J]. Brazilian Journal of Chemical Engineering, 2014, 31: 571-590.

[9]. LI Q., YUN Q., WANG K., et al. Surface engineering construction mode and process technologies for medium and high maturity shale oil and tight oil[J]. Petroleum and New Energy, 2021, 33(3): 82–89.

[10]. Hou L., Yu Z., Luo X., et al. Key geological factors controlling the estimated ultimate recovery of shale oil and gas: A case study of the Eagle Ford shale, Gulf Coast Basin, USA[J]. Petroleum Exploration and

Development, 2021, 48(3): 762-774.

[11]. Zhang L., Wang Z., Wang Q., et al. Simulation of oil shale semi-coke particle cold transportation in a spouted bed using CPFD method[J]. Powder Technology, 2016, 301: 360-368.

[12]. Lyu Y., Huang Q., Liu L., et al. Experimental and molecular dynamics simulation investigations of adhesion in heavy oil/water/pipeline wall systems during cold transportation[J]. Energy, 2022, 250: 123811.

[13]. Coskuner G., Naderi K., Babadagli T.. An enhanced oil recovery technology as a follow up to cold heavy oil production with sand[J]. Journal of Petroleum Science and Engineering, 2015, 133: 475-482.

[14]. Margarone M., Bennardo A., Busto. C, Correra S.. Waxy oil pipeline transportation through cold flow technology: rheological and pressure drop analyses[J]. Energy Fuels, 2013, 27: 1809−1816.

[15]. Adeyanju O., Oyekunle L.. An experimental study of rheological properties of Nigerian waxy crude oil[J]. Petroleum Science and Technology, 2012, 30: 1102-1111

[16]. Sun G., Zhang J., Li H.. Structural behaviors of waxy crude oil emulsion gels[J]. Energy Fuels, 2014, 28: 3718−3729.

[17]. Yao B., Li C., Yang F., et al. Structural properties of gelled Changqing waxy crude oil benefitted with nanocomposite pour point depressant[J]. Fuel, 2016, 184: 544-554.

[18]. U. Srilakshmi, J Manikandan, Thanmayee Velagapudi, Gandla Abhinav, Tharun Kumar, & Dogiparthy Saideep. (2024). A New Approach to Computationally- Successful Linear and Polynomial Regression Analytics of Large Data in Medicine. Journal of Computer Allied Intelligence, 2024, *2*(2): 35-48.

[19]. Adeyanju O. A., Oyekunle L. O.. Experimental study of water-in-oil emulsion flow on wax deposition in subsea pipelines[J]. Journal of Petroleum Science and Engineering, 2019, 182: 106294.

[20]. Yao Z., Zhang Y., Zheng Y., et al. Enhance flows of waxy crude oil in offshore petroleum pipeline: A review[J]. Journal of Petroleum Science and Engineering, 2022, 208: 109530.

[21]. Zhang Z., Li J., Wang Z., et al. Preparation and performance characterization of a novel high-performance epoxy resin modified reactive liquid asphalt[J]. Construction and Building Materials, 2020, 263: 120113.

[22]. Srinivasa Sai Abhijit Challapalli. Optimizing Dallas-Fort Worth Bus Transportation System Using Any Logic. *Journal of Sensors, IoT & Health Sciences*, 2024, *2*(4):40-55.

[23]. Souas F., Safri A., Benmounah A.. A review on the rheology of heavy crude oil for pipeline transportation[J]. Petroleum Research, 2021, 6(2): 116-136.

[24]. Marinho T. O., De Oliveira M. C. K., Nele M.. Experimental investigation of the rheology and crystal morphology of model waxy oils under gelling conditions[J]. Energy & Fuels, 2019, 33(10): 9604-9618.

[25]. Dong H., Zhao J., Wei L., et al. Effect of initial cooling temperature on structural behaviors of gelled waxy crude oil and microscopic mechanism investigation[J]. Energy & Fuels, 2020, 34(12): 15782-15801.

[26]. Liu Z., Li Y., Wang W., et al. Wax and wax–hydrate deposition characteristics in single-, two-, and three-phase pipelines: a review[J]. Energy & Fuels, 2020, 34(11): 13350-13368.

[27]. Aiyejina A., Chakrabarti D. P., Pilgrim A., et al. Wax formation in oil pipelines: A critical review[J]. International journal of multiphase flow, 2011, 37(7): 671-694.

[28]. Zheng S., Saidoun M., Palermo T., et al. Wax deposition modeling with considerations of non-Newtonian

characteristics: Application on field-scale pipeline[J]. Energy & Fuels, 2017, 31(5): 5011-5023.

[29]. Vryzas Z., Kelessidis V. C.. Nano-based drilling fluids: A review[J]. Energies, 2017, 10(4): 540.

[30]. Chi Y., Yang J., Sarica C., et al. A critical review of controlling paraffin deposition in production lines using chemicals[J]. Energy & fuels, 2019, 33(4): 2797-2809.

[31]. Li W., Li H., Da H., et al. Influence of pour point depressants (PPDs) on wax deposition: A study on wax deposit characteristics and pipeline pigging[J]. Fuel Processing Technology, 2021, 217: 106817.

[32]. Moncayo-Riascos I., Taborda E., Hoyos B. A., et al. Effect of resin/asphaltene ratio on the rheological behavior of asphaltene solutions in a de-asphalted oil and p-xylene: A theoretical–experimental approach[J]. Journal of Molecular Liquids, 2020, 315: 113754.

[33]. Leela Vathy.B, & RamMohan Rao Kovvur. Deep Convolutional Neural Network (DEEP-CNN) for Multi-Class Classification of Biotic Stress in Paddy Crop. Journal of Computer Allied Intelligence, 2025, *3*(1): 18-30.

[34]. Wang Z., Bai Y., Zhang H., et al. Investigation on gelation nucleation kinetics of waxy crude oil emulsions by their thermal behavior[J]. Journal of Petroleum Science and Engineering, 2019, 181: 106230.

[35]. Xue Y., Zhao Z., Xu G., et al. Effect of poly-alpha-olefin pour point depressant on cold flow properties of waste cooking oil biodiesel blends[J]. Fuel, 2016, 184: 110-117.

[36]. Shasha H., Qiyu H.. Research on wax deposition in the pipeline without pigging for a long time[J]. Petroleum science and technology, 2014, 32(3): 316-323.